Supporting Information

Pd-Ru Nanocatalysts Derived from a Pd-Induced Aerogel for Dramatic Boosting of Hydrogen Release

Xiaojiao Yang,[a] Jianyu Wei,[ab] Qi Wang,[b] Maobin Shuai,*[a] Guozong Yue,[a] Peilong Li,[a] Deshun Huang,[a] Didier Astruc,[b] and Pengxiang Zhao*[a]

Chemicals and Materials

All commercial chemicals and regents were used without further purification in this work.

Na_2PtCl_6 $6H_2O$ (98%), Poly(vinyl alcohol) (PVA) with a degree of hydrolysis of 80% and Mw of 8,000 - 10,000 were purchased from Sigma and Aldrich Company (UK). The chemical reagents *N, N'*-carbonyldiimidazole (CDI) (97%), propargylamine (98%), Na_2PdCl_4 (98%), $PdCl_2$ (Pd 59-60%), NaOH (AR), $FeCl_3$ (98%), $CoCl_2$ (99.7%), $NiCl_2$ (98%), $CuSO_4$, $NaBH_4$ (99%), $H_3N\text{-}BH_3$, HCl (36%), KOH (AR), MoS_2 and organic solvents were supplied by Aladdin Co., Ltd. $RuCl_3$ $RhCl_3{\cdot}3H_2O$ (Rh 38.5-42.5%), $HAuCl_4{\cdot}3H_2O$ (99%) were purchased from Shanghai Macklin Biochemical Co., Ltd.

Milli-Q water (18.2 MΩ) was used for all the nanoparticle preparations.

Experiment Section

Preparation of Pd(II)@Alkyne-PVA aerogel(ZZM-1): 100 mg Alkynes-PVA was dissolved in 1.6 mL DMF in a vial. 10 mg Na_2PdCl_4 was dissolved in the mixture of DMF and HCl aqueous solution (pH = 1.0) (400 μL, 1:1, v/v). The Na_2PdCl_4 solution was dropped into Alkynes-PVA solution and mixed to obtain a homogenized mixture. The resulting solution was sealed to form a gel. The wet gel was subjected to solvent exchange with 15 mL deionized water for 24 h. After freezing dry yellow aerogel was obtained.

Preparation of the *Nanocatalysts (*Pd_1Ru_2NPs@Alkyne-PVA gel as Example*)*: A Schlenk tube was charged with 100 mg Pd(II)@Alkyne-PVA gel under N_2. Then 5 mL water was injected, and the mixture was sonicated for 5 min and allowed to stir for an hour under N_2. The $RuCl_3$ (14.1 mg, 0.068 mmol) dissolved in 2 mL water was injected (the molar ratio of the Pd:Ru were 1:2). This mixture was stirred continuously at room temperature for 2 h. Then 2 mL aqueous solution of fresh prepared $NaBH_4$ (38.6 mg, 1.02 mmol) was quickly added after degassing with N_2 for 5 min. The mixture was allowed to further stir for another 30 min, and the resulting nanocatalyst was collected by centrifugation, washed with water and dried at 60 °C in vacuo overnight. The metal content was quantified by inductively coupled plasma atomic emission spectroscopy (ICP-AES). A similar synthetic process was used for various other Ru/Pd ratios.

Hydrolysis reaction of Ammonia Borane (AB): The hydrogen evolution reactions of AB were conducted in water at certain temperature. In a 50 mL Schlenk flask, 1 mol% nanocatalyst (measured by ICP-OES) was dissolved in 5 mL water with continuous stirring. 15.4 mg (0.5 mmol) AB was dissolved in 1 mL water then injected in the flask, and timing started. The flask is connected via a gas outlet to a water-filled gas burette. The amount of gas evolved is recorded periodically by measuring the displacement of water in the burette. In this case, a quantitative conversion of AB produces 3.0 equivalents of H_2 occupying ca. 33.5 mL at atmospheric pressure. Prior to the hydrolysis reactions, the volumes are measured at atmospheric pressure and corrected for water vapor pressure at room temperature.

Hydrogenation of styrene with hydrogen generated from AB hydrolysis: 14 mg (1 mmol% per AB) Pd_1Ru_2NPs@Alkyne-PVA gel was added into the left tube. Meanwhile 10.5 mg (1.5 mmol% per styrene) was added into the right tube. After removed the air in vacuo, 2 mL methanol with 52 mg (0.5 mmol) styrene was added into the right tube. Then 30.87 mg (1 mmol) AB dissolved in 2 mL D_2O was added into the left tube. After stirring for 2 min, the system was heated in oil bath at 50 ^{o}C. After 12 hours, the reaction solution in the right tube was collected by centrifugation for GC-MS analysis without any further treatment.

Characterization

The microstructures of the nanocatalysts were characterized with transmission electron microscopy (TEM) by Zessi Libra 200FE. High angle annular dark field scanning transmission electron microscopy (HAADFTEM) was performed on a Thermo Fisher Titan Themis, 60-300 ‘‘cubed’’ microscope fitted with aberration-correctors for the imaging lens and the probe forming lens, Super-X EDX system, operated at 300 kV.

X-ray photoelectron spectroscopy (XPS) analysis was performed on a Escalab 250Xi XPS system with an Al Ka X-ray source (1486.6 eV photons).

The concentration of metal ions in the gels was carried out on an iCAP 7200 ICP-OES.

Gas Chromatography-Mass Spectrometer (GC-MS) was performed by Angilent 5977A.

Characterization of catalysts

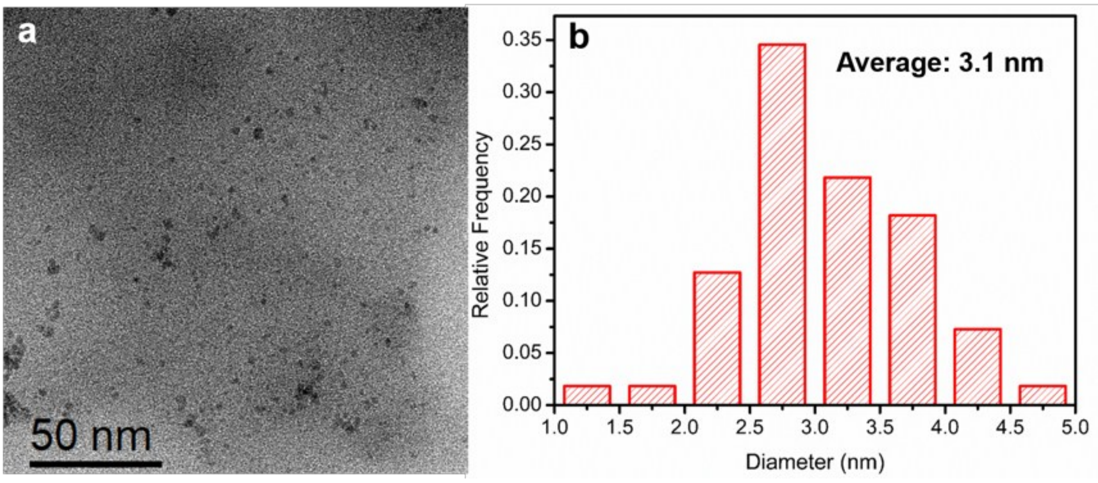

Figure S1. The TEM image (a) and size distributions (b) of Pd_3Ru_1NPs@Alkyne-PVA gel.

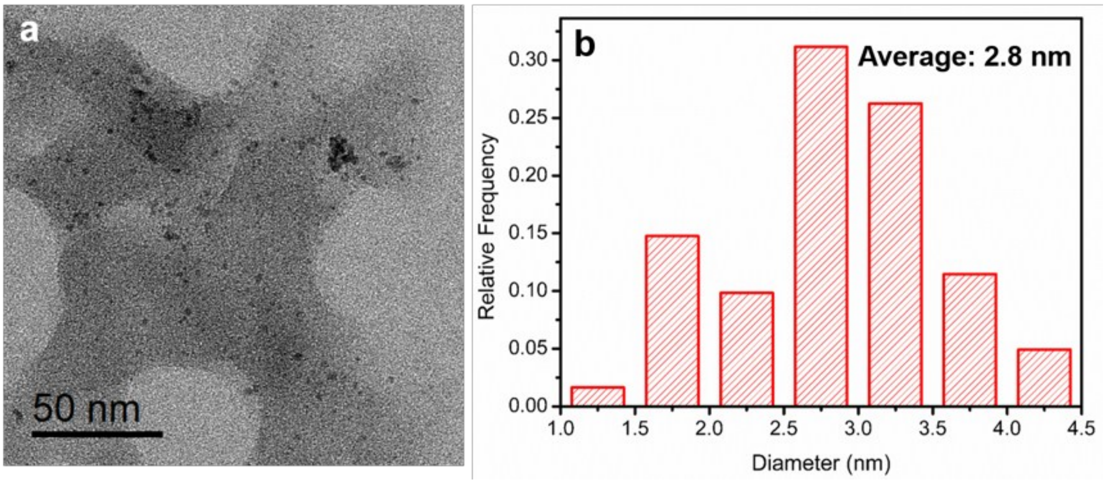

Figure S2. The TEM image (a) and size distributions (b) of Pd_2Ru_1NPs@Alkyne-PVA gel.

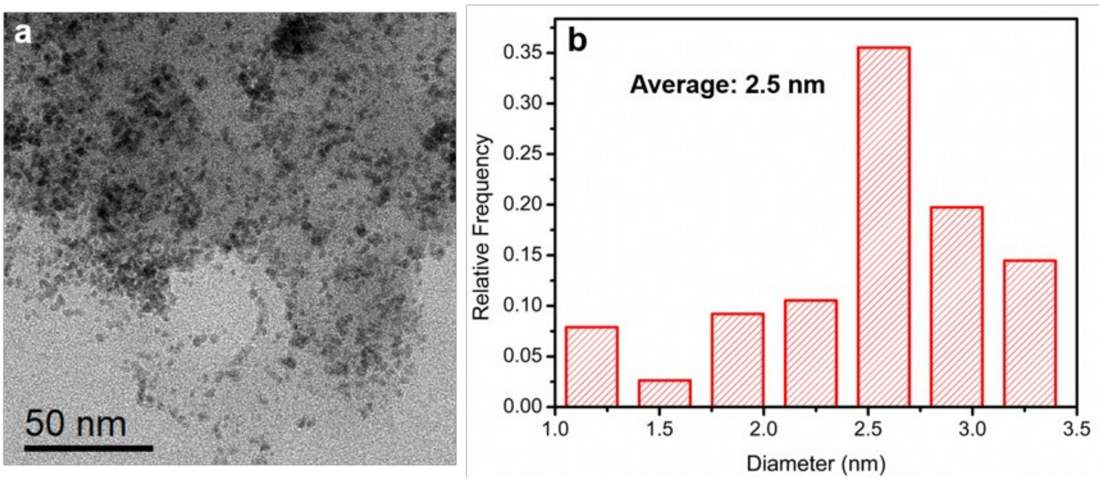

Figure S3. The TEM image (a) and size distributions (b) of Pd_1Ru_1NPs@Alkyne-PVA gel.

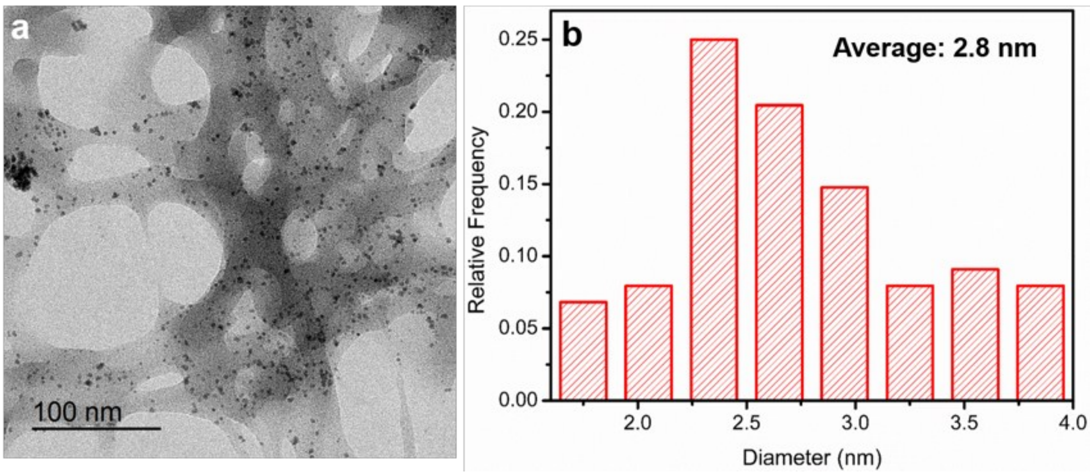

Figure S4. The TEM image (a) and size distributions (b) of Pd_1Ru_3NPs@Alkyne-PVA gel.

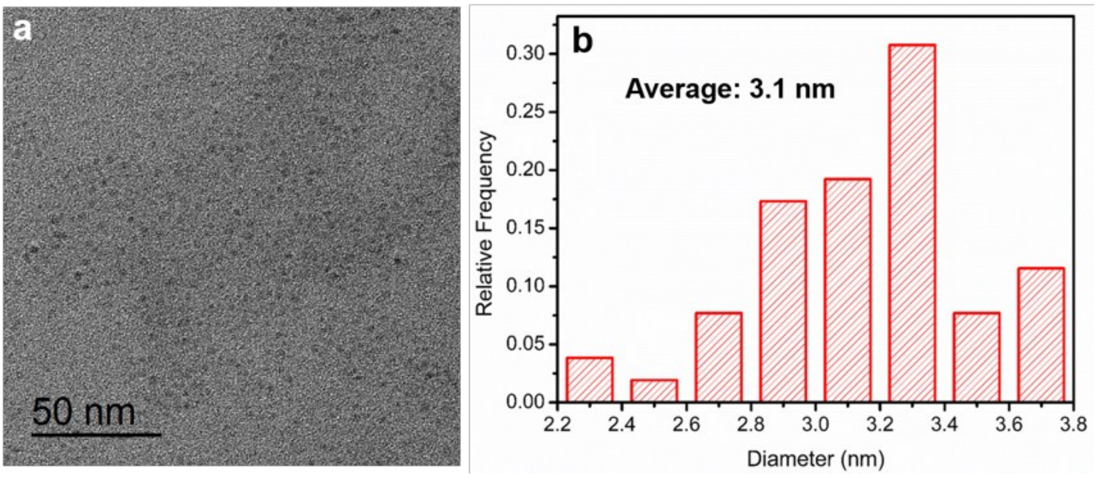

Figure S5. The TEM image (a) and size distributions (b) of PdNPs@Alkyne-PVA gel.

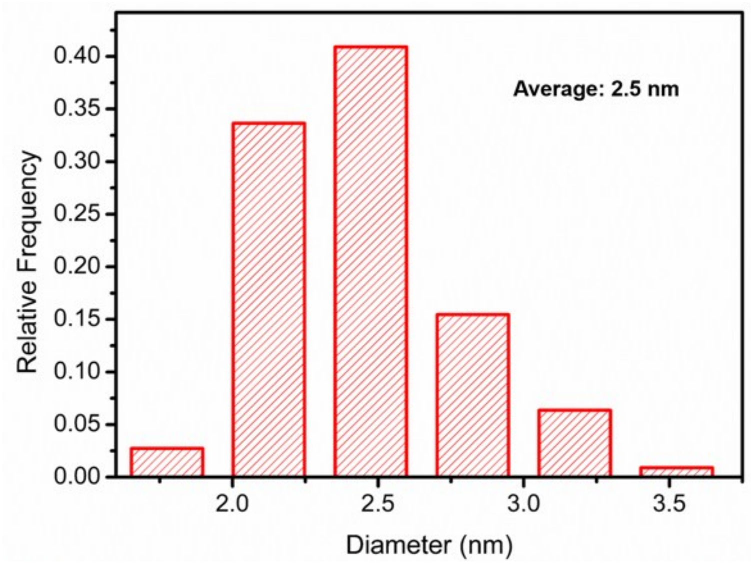

Figure S6. The size of Pd_1Ru_2 nanoparticles in the Pd_1Ru_2NPs@Alkyne-PVA gel network.

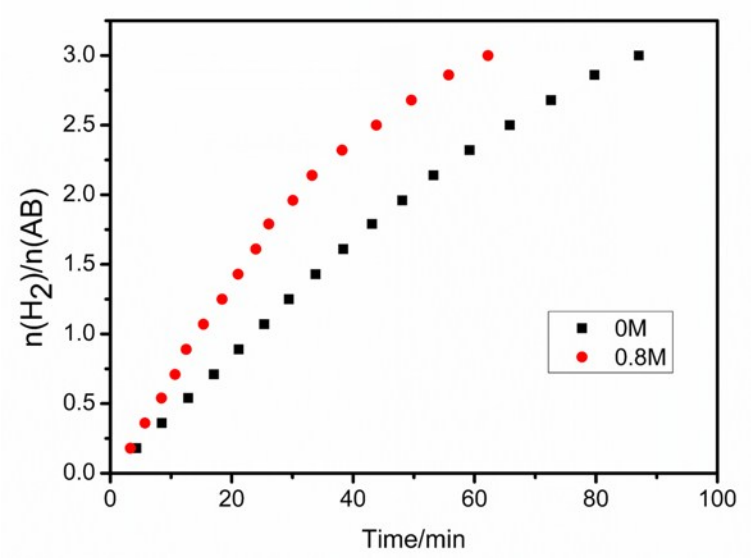

Figure S7. 1 mol % PdNPs@Alkyne-PVA gel catalyzed hydrogen evolution form NH_3BH_3 hydrolysis

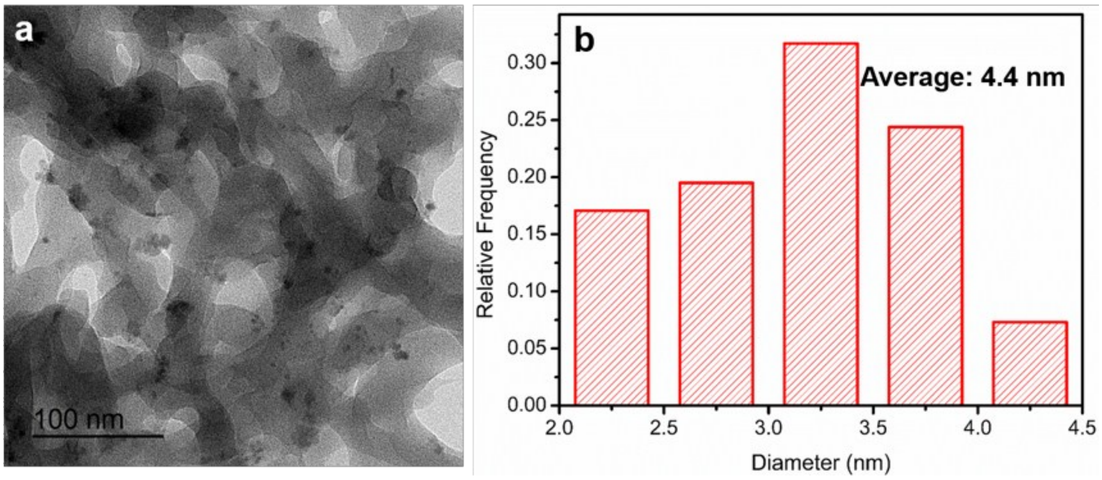

Figure S8. The TEM image (a) and size distributions (b) of Pd_1Fe_2NPs@Alkyne-PVA gel.

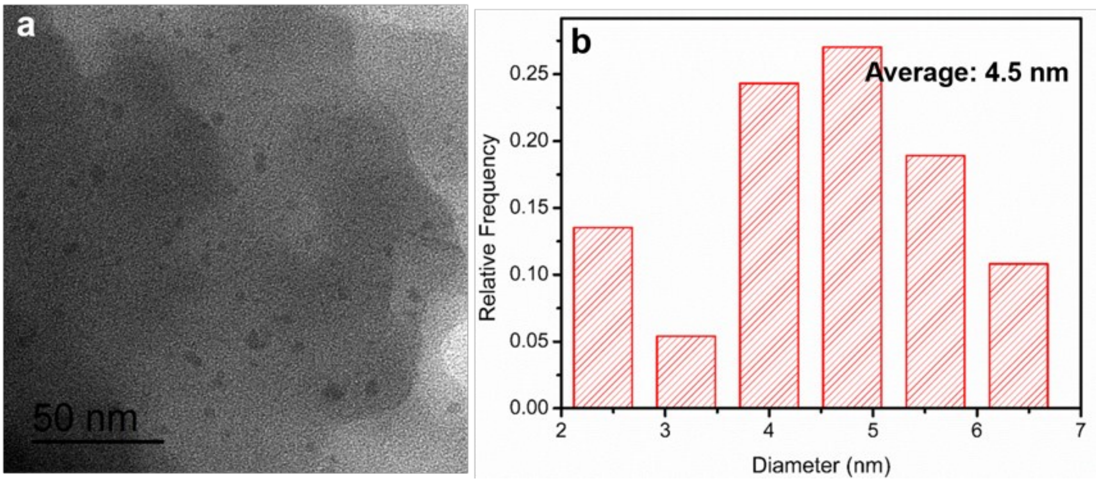

Figure S9. The TEM image (a) and size distributions (b) of Pd_1Co_2NPs@Alkyne-PVA gel.

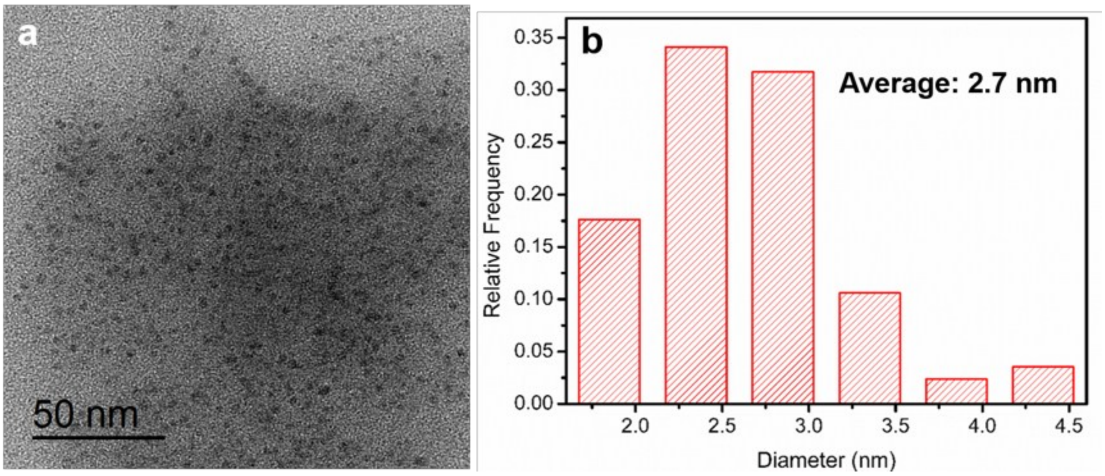

Figure S10. The TEM image (a) and size distributions (b) of Pd_1Ni_2NPs@Alkyne-PVA gel.

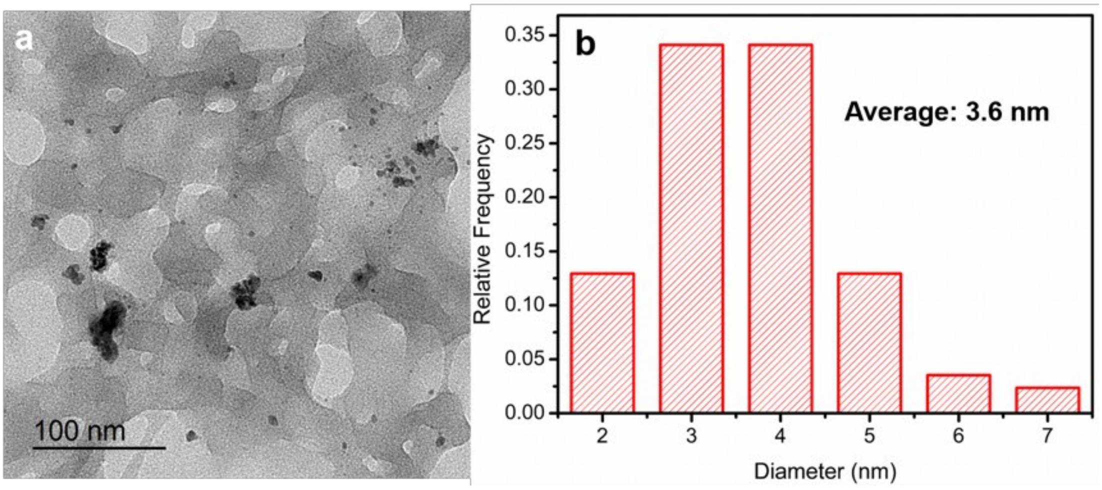

Figure S11. The TEM image (a) and size distributions (b) of Pd_1Cu_2NPs@Alkyne-PVA gel.

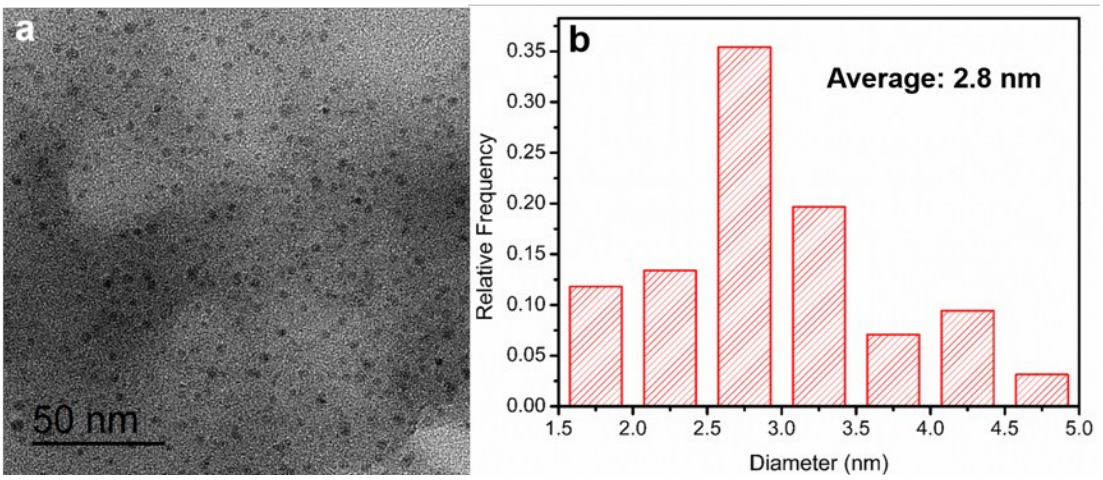

Figure S12. The TEM image (a) and size distributions (b) of Pd_1Au_2NPs@Alkyne-PVA gel.

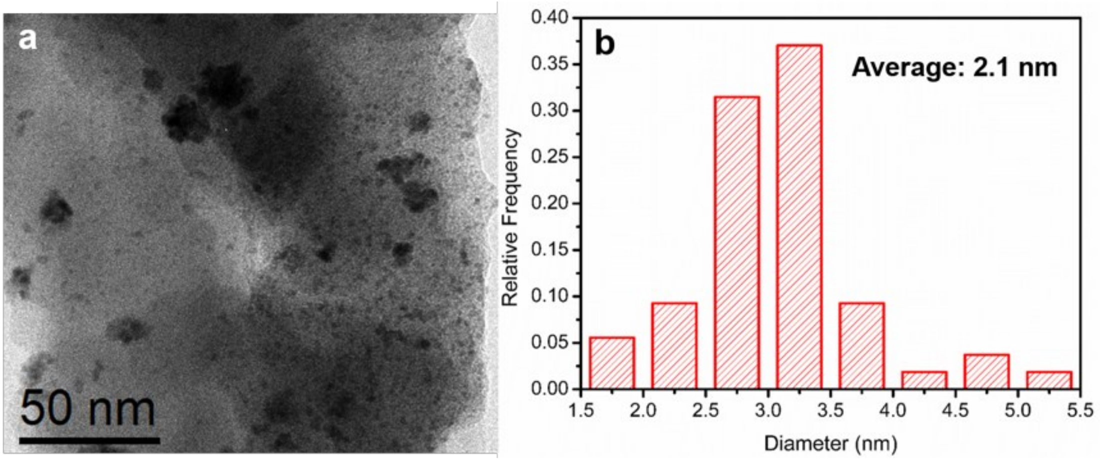

Figure S13. The TEM image (a) and size distributions (b) of Pd_1Pt_2NPs@Alkyne-PVA gel.

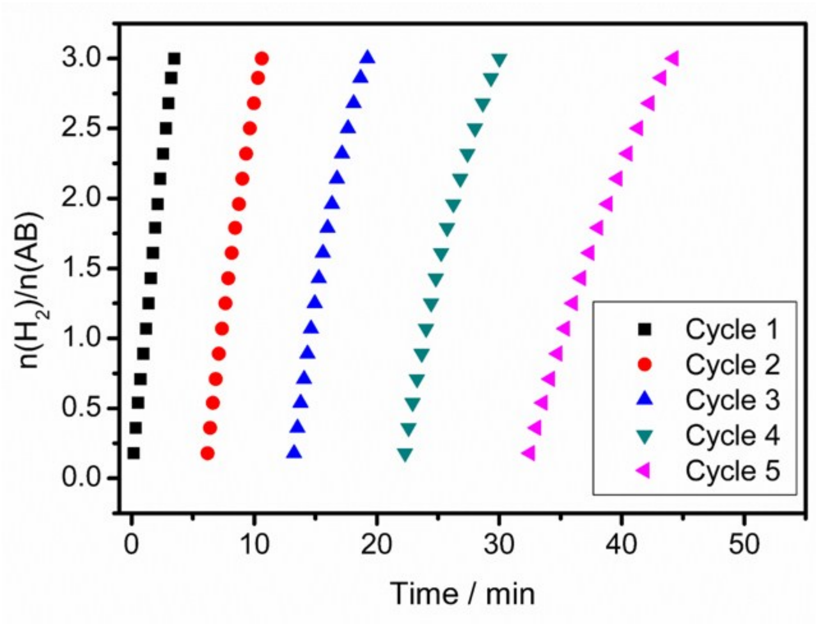

Figure S14. Plots of the volume of hydrogen vs time for AB hydrolysis catalyzed by 1 mol % Pd_1Ru_2NPs@Alkyne-PVA gel during the tests of reusability.

Table S1. Physical properties and comparison of the catalytic efficiency of Pd_xRu_yNPs@Alkyne-PVA gel.

Catalyst	Size [a] (nm)	Atomic ratios [b]	Metal loadings (wt%) [b]	R(nm) [c]	Ns/N [d]	TOFt [e]	TOF [f]
PdNPs @Alkyne-PVA gel	3.1	-	7.2	0.14	36%	3.45/4.82 [g]	9.54/13.35 [g]
Pd_3Ru_1NPs@Alkyne-PVA gel	3.1	3.4:1	4.7	0.138	36%	68.49/136.36 [g]	192.33/382.91 [g]
Pd_2Ru_1NPs@ Alkyne-PVA gel	2.8	2.2:1	5.5	0.137	39%	79.63/158.73 [g]	196.52/405.52 [g]
Pd_1Ru_1NPs@Alkyne-PVA gel	2.5	1.2:1	6.4	0.135	43%	77.92/206.90 [g]	180.38/478.93 [g]
Pd_1Ru_2NPs@Alkyne-PVA gel	2.5	1:1.5	7.4	0.134	43%	86.21/247.93 [g]	201.04/578.20 [g]
Pd_1Ru_3NPs@Alkyne-PVA gel	2.8	1:2.3	10.2	0.133	38%	43.29/126.58 [g]	113.92/333.11 [g]

[a] Average size of nanoparticle; [b] Measured by ICP-OES; [c] Average radius of atom; [d] Ns/N = Number of surface atoms / Number of total atoms; [e] $TOF^t = mol_{H2}$ released / (total molcatalyst × reaction time(min)); [f] TOF = TOFt / (Ns/N); [g] TOF obtained in the presence of 0.8M NaOH.

Table S2. Physical properties and comparison of the catalytic efficiency of Bimetallic NPs@Alkyne-PVA gel catalysts.

Catalyst	Size [a] (nm)	Atomic ratios [b]	Metal loadings (wt%) [b]	R(nm) [c]	Ns/N [d]	TOFt [e]	TOF [f]
Pd_1Ru_2NPs@ Alkyne-PVA gel	2.5	1:1.5	7.4	0.134	43%	86.21/247.93 [g]	201.04/578.20 [g]
Pd_1Ru_3NPs@ Alkyne-PVA gel	2.8	1:2.3	10.2	0.133	38%	43.29/126.58 [g]	113.92/333.11 [g]
Pd_1Fe_2NPs@ Alkyne-PVA gel	4.4	1:1.5	5.9	0.140	25%	5.78/13.57 [g]	22.71/53.33 [g]
Pd_1Co_2NPs@ Alkyne-PVA gel	4.5	1:1.9	6.1	0.138	25%	12.53/26.11 [g]	51.08/106.43 [g]
Pd_1Ni_2NPs@ Alkyne-PVA gel	2.7	1:2.07	6.4	0.138	41%	3.59/7.02 [g]	8.77/17.16 [g]
Pd_1Cu_2NPs@ Alkyne-PVA gel	3.6	1:2.2	6.8	0.138	31%	3.15/3.86 [g]	10.27/12.58 [g]
Pd_1Au_2NPs@ Alkyne-PVA gel	2.8	1:1.8	12.8	0.138	49%	10.09/26.39 [g]	25.58/66.92 [g]
Pd_1Pt_2NPs@ Alkyne-PVA gel	2.1	1:1.87	12.9	0.138	53%	65.65/85.96 [g]	124.87/163.51 [g]

[a] Average size of nanoparticle; [b] Measured by ICP-OES; [c] Average radius of atom; [d] Ns/N = Number of surface atoms / Number of total atoms; [e] $TOF^t = mol_{H2}$ released / (total molcatalyst × reaction time(min)); [f] TOF = TOFt / (Ns/N); [g] TOF obtained in the presence of 0.8M NaOH.

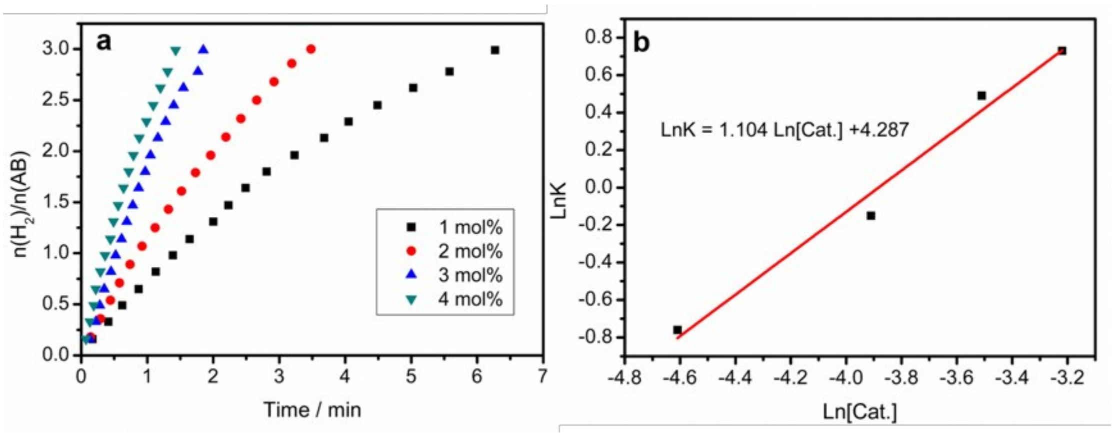

Figure S15. (a) Plots of the times of the catalyzed AB hydrolytic dehydrogenation catalyzed by the Pd_1Ru_2NPs@Alkyne-PVA gel with various catalyst amounts. (b) Plots of the rates of H_2 generation vs the concentration of the Pd_1Ru_2NPs@Alkyne-PVA gel both on natural logarithmic scales.

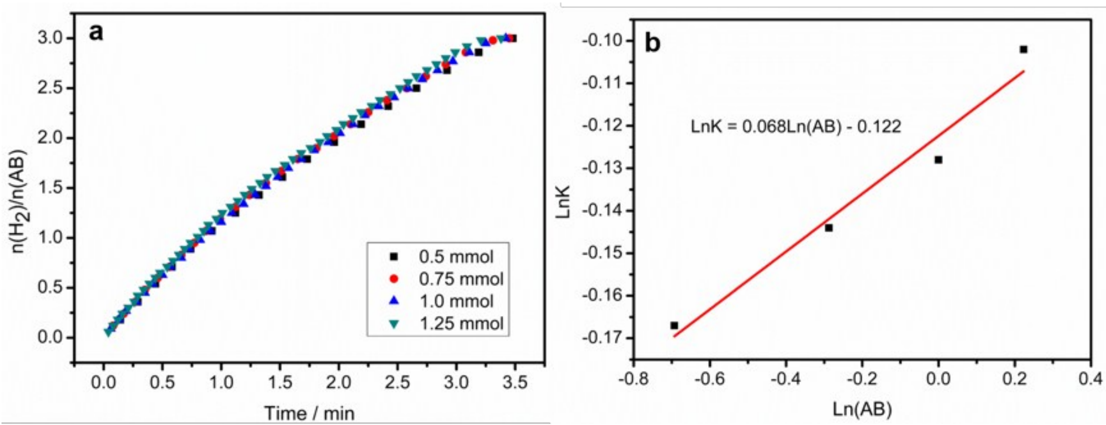

Figure S16. (a)Plots of the volume of hydrogen generated vs time for the hydrolysis of AB catalyzed by 1 mol % Pd_1Ru_2NPs@Alkyne-PVA gel. (b) Plots of the H_2 generation rate vs AB concentration both on natural logarithmic scales.

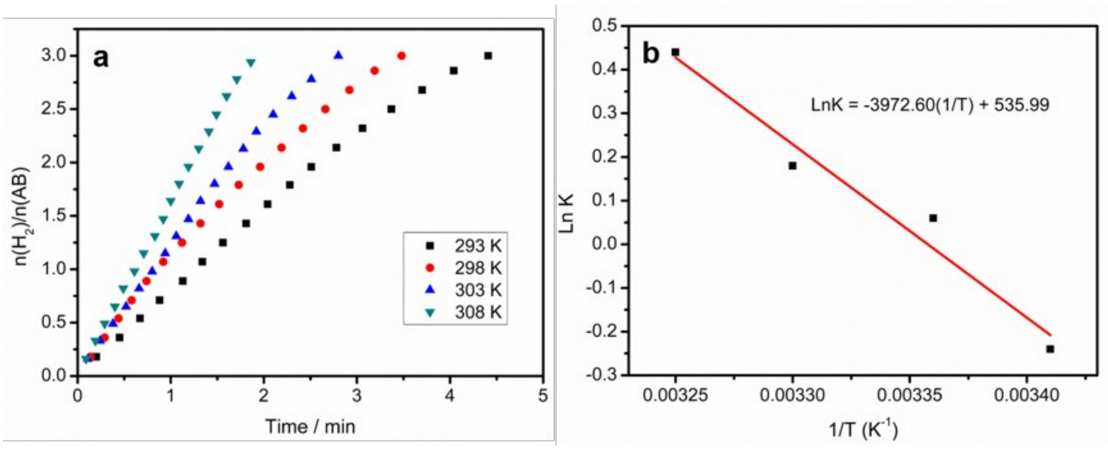

Figure S17. (a) Plots of the hydrogen volume vs time for AB hydrolysis catalyzed at various temperatures by 1 mol % Pd_1Ru_2NPs@Alkyne-PVA gel. (b) Kinetic data obtained from the Arrhenius plots.

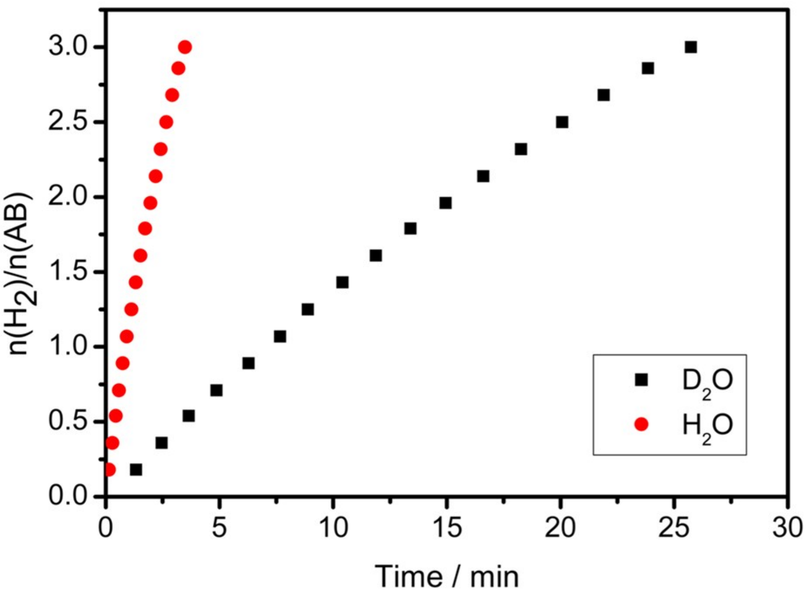

Fig. S18 Hydrogen generation upon NH_3BH_3 hydrolysis with H_2O and D_2O catalyzed by 1 mol % nanocatalyst Pd_1Ru_2NPs@Alkyne-PVA gel (KIE = 7.29).

Figure S19. The sealed communicating vial for the tandem reaction.

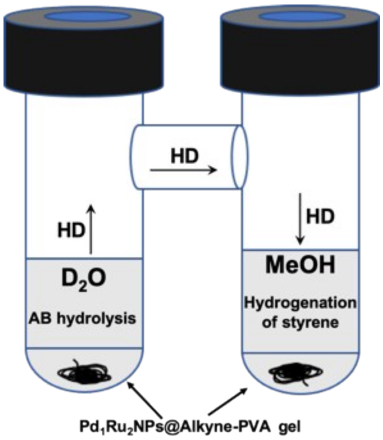

Figure S20. Tandem reaction for hydrogenation with “HD” generated from AB hydrolysis catalyzed by Pd_1Ru_2NPs@Alkyne-PVA gel.

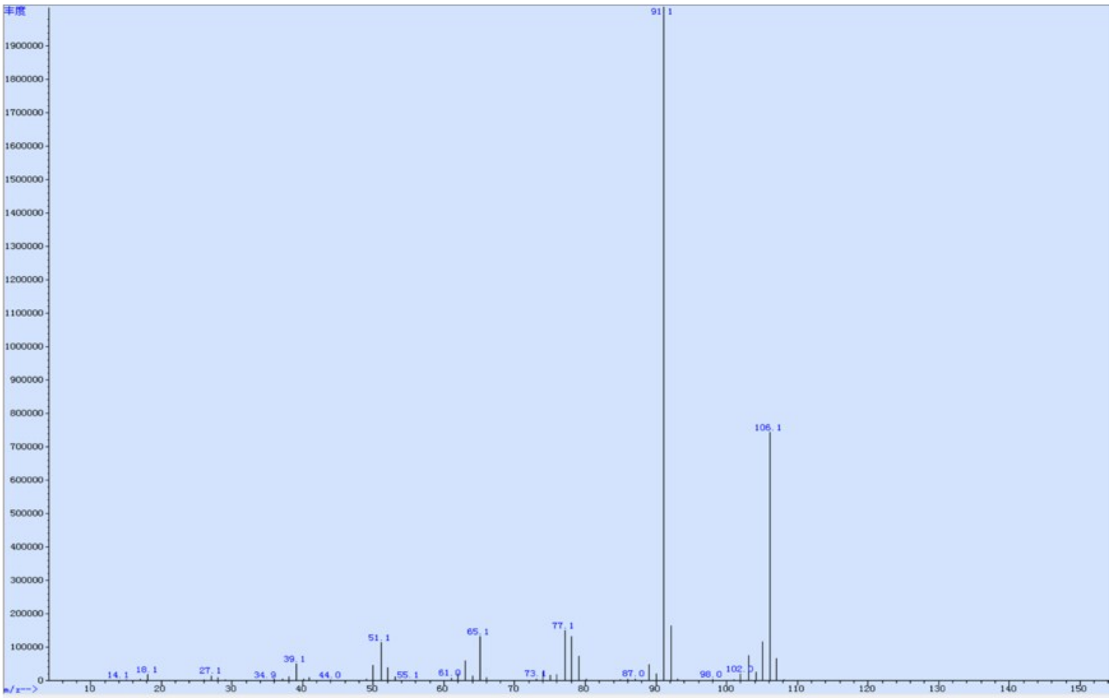

Fig S21. The GC-MS analysis of ethylbenzene. m/z 106 ($C_6H_5CH_2CH_3$).

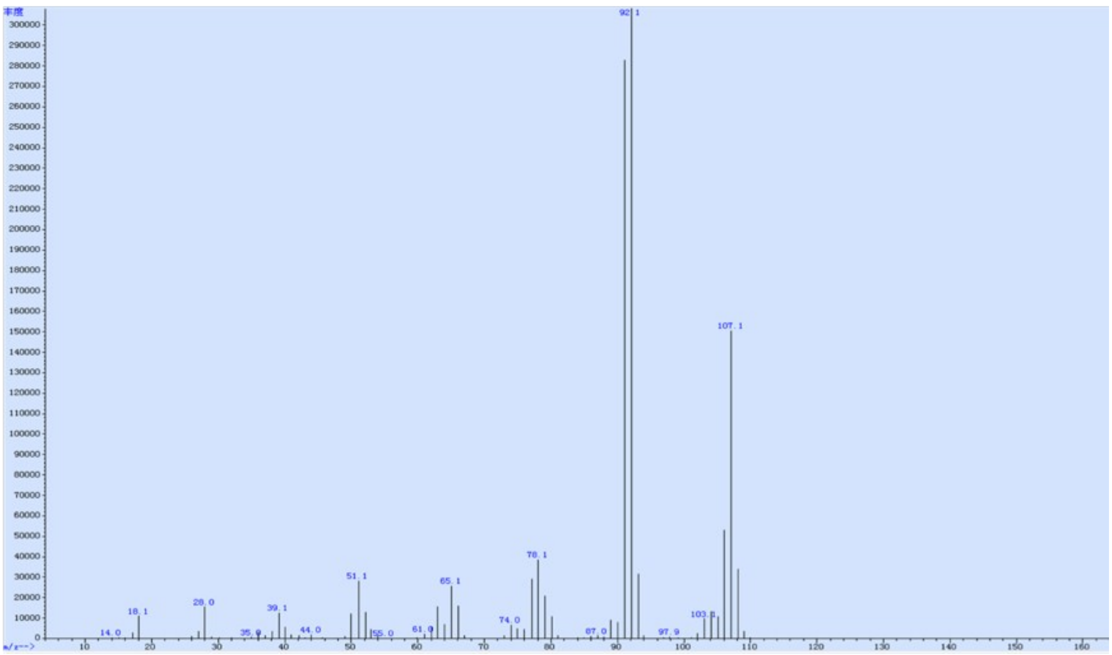

Figure S22. The GC-MS analysis of ethylbenzene. m/z 106 ($C_6H_5CH_2CH_3$), 107 ($C_6H_5CHDCH_3$, $C_6H_5CHCH_2D$), 108 ($C_6H_5CHDCH_2D$).

.

Table S3. Comparison the catalytic activity of the Ru-based catalysts for AB hydrolysis reported in the literature.

Catalyst	Temperature (℃)	Catalyst/AB (molar ratio)	TOF (mol_{H2} mol_{cat}^{-1} min^{-1})	Reference
Pd_1Ru_2NPs@Alkyne-PVA gel	25	0.01	578.2	This work
Pt-Ru@PVP NPs	25	0.003	308	S1
PtRu	25	0.001	59.6	S2
PtPd cNPs	25	0.002	50.02	S3
PtRu/C	25	0.03	8	S4
Ru/ND	25	0.003	229	S5
Ru/HPCM	30	0.003	440	S6
Ru(0)/MIL-96	25	0.0039	231	S7
Pd NPs/CS-rGO	30	-	42.5	S8
PdNi/MIL-101	25	-	76(based-Pd)	S9
Pd@Co/graphene	rt	0.002[a]	408.9(based on Pd)	S10
Ru@Co/graphene	25	0.004[b]	344(Based on Ru)	S11
CoPd/C annealed	25	0.024	35.7	S12
Ru@MIL-53(Cr)	rt	0.004	260.8	S13
Pd/CeO_2	25	0.011	29	S14
CuPd/RGO	25	-	19.9	S15
PdNi/rGO	25	0.01	28.3	S16
PdNPs-Cs-rGO	30	-	42.5	S17
3wt%Pt-3 wt%Ru/CNT	25	-	547	S18

Reference

1. M. Rakap, Hydrogen generation from hydrolysis of ammonia borane in the presence of highly efficient poly (N-vinyl-2-pyrrolidone)-protected platinum-ruthenium nanoparticles[J]. *Appli. Catal. A: Gen.*, 2014, **478,** 15-20.
2. Q. Zhou, C. Xu, *Chem. - Asian J.*, 2016, 11, 705-712.
3. Amali, A. J.; Aranishi, K.; Uchida, T.; Xu, Q. Part. Part. Syst. Charact. 2013, 30, 888-892.
4. Yao, C. F.; Zhuang, L.; Cao, Y. L.; Ai, X. P.; Yang, H. X. Int. J. Hydrogen Energy, 2008, 33, 2462-2467.

5. Fan G, Liu Q, Tang D, et al. Nanodiamond supported Ru nanoparticles as an effective catalyst for hydrogen evolution from hydrolysis of ammonia borane[J]. International Journal of Hydrogen Energy, 2016, 41(3): 1542-1549.
6. Zhong F, Wang Q, Xu C, et al. Ultrafine and highly dispersed Ru nanoparticles supported on nitrogen-doped carbon nanosheets: Efficient catalysts for ammonia borane hydrolysis[J]. Applied Surface Science, 2018, 455: 326-332.
7. Wen L, Su J, Wu X, et al. Ruthenium supported on MIL-96: an efficient catalyst for hydrolytic dehydrogenation of ammonia borane for chemical hydrogen storage[J]. International Journal of Hydrogen Energy, 2014, 39(30): 17129-17135.
8. Liu S, Chen X, Wu Z J, et al. Chitosan-reduced graphene oxide hybrids encapsulated Pd (0) nanocatalysts for H2 generation from ammonia borane[J]. International Journal of Hydrogen Energy, 2019, 44(42): 23610-23619.
9. Du Y, Wang K, Zhai Q, et al. Alloyed palladium-nickel hollow nanospheres with interatomic charge polarization for improved hydrolytic dehydrogenation of ammonia borane[J]. International Journal of Hydrogen Energy, 2018, 43(1): 283-292.
10. Wang J, Qin Y L, Liu X, et al. In situ synthesis of magnetically recyclable graphene-supported Pd@ Co core–shell nanoparticles as efficient catalysts for hydrolytic dehydrogenation of ammonia borane[J]. Journal of Materials Chemistry, 2012, 22(25): 12468-12470.
11. Cao N, Su J, Luo W, et al. Graphene supported Ru@ Co core–shell nanoparticles as efficient catalysts for hydrogen generation from hydrolysis of ammonia borane and methylamine borane[J]. Catalysis Communications, 2014, 43: 47-51.
12. Sun D, Mazumder V, Metin O, et al. Catalytic hydrolysis of ammonia borane via cobalt palladium nanoparticles[J]. ACS nano, 2011, 5(8): 6458-6464.
13. Yang K, Zhou L, Yu G, et al. Ru nanoparticles supported on MIL-53 (Cr, Al) as efficient catalysts for hydrogen generation from hydrolysis of ammonia borane[J]. International Journal of Hydrogen Energy, 2016, 41(15): 6300-6309.
14. Abo-Hamed E K, Pennycook T, Vaynzof Y, et al. Highly active metastable ruthenium nanoparticles for hydrogen production through the catalytic hydrolysis of ammonia borane[J]. Small, 2014, 10(15): 3145-3152.
15. Güngörmez K, Metin Ö. Composition-controlled catalysis of reduced graphene oxide supported CuPd alloy nanoparticles in the hydrolytic dehydrogenation of ammonia borane[J]. Applied Catalysis A: General, 2015, 494: 22-28.

16. Çiftci N S, Metin Ö. Monodisperse nickel–palladium alloy nanoparticles supported on reduced graphene oxide as highly efficient catalysts for the hydrolytic dehydrogenation of ammonia borane[J]. International Journal of Hydrogen Energy, 2014, 39(33): 18863-18870.
17. Liu S, Chen X, Wu Z J, et al. Chitosan-reduced graphene oxide hybrids encapsulated Pd (0) nanocatalysts for H2 generation from ammonia borane[J]. International Journal of Hydrogen Energy, 2019, 44(42): 23610-23619.
18. Chen W, Li D, Peng C, et al. Mechanistic and kinetic insights into the Pt-Ru synergy during hydrogen generation from ammonia borane over PtRu/CNT nanocatalysts[J]. Journal of catalysis, 2017, 356: 186-196.